

Article

Discovery of Potent, Efficient and Selective Inhibitors of Phosphoinositide 3-Kinase β Through a Deconstruction and Regrowth Approach.

Nick Barton, Maire A. Convery, Anthony W.J. Cooper, Kenneth David Down, Nicole Hamblin, Graham Inglis, Simon Peace, James E. Rowedder, Paul Rowland, Jonathan A Taylor, and Natalie Wellaway

J. Med. Chem., **Just Accepted Manuscript** • DOI: 10.1021/acs.jmedchem.8b01556 • Publication Date (Web): 11 Dec 2018

Downloaded from <http://pubs.acs.org> on December 11, 2018

Just Accepted

"Just Accepted" manuscripts have been peer-reviewed and accepted for publication. They are posted online prior to technical editing, formatting for publication and author proofing. The American Chemical Society provides "Just Accepted" as a service to the research community to expedite the dissemination of scientific material as soon as possible after acceptance. "Just Accepted" manuscripts appear in full in PDF format accompanied by an HTML abstract. "Just Accepted" manuscripts have been fully peer reviewed, but should not be considered the official version of record. They are citable by the Digital Object Identifier (DOI®). "Just Accepted" is an optional service offered to authors. Therefore, the "Just Accepted" Web site may not include all articles that will be published in the journal. After a manuscript is technically edited and formatted, it will be removed from the "Just Accepted" Web site and published as an ASAP article. Note that technical editing may introduce minor changes to the manuscript text and/or graphics which could affect content, and all legal disclaimers and ethical guidelines that apply to the journal pertain. ACS cannot be held responsible for errors or consequences arising from the use of information contained in these "Just Accepted" manuscripts.

Discovery of Potent, Efficient and Selective Inhibitors of Phosphoinositide 3-Kinase δ Through a
Deconstruction and Regrowth Approach.

Nick Barton, Maire Convery, Anthony W. J. Cooper, Kenneth Down*, J. Nicole Hamblin[§], Graham Inglis,
Simon Peace, James Rowedder, Paul Rowland, Jonathan A. Taylor and Natalie Wellaway.

GlaxoSmithKline R&D, Medicines Research Centre, Gunnels Wood Road, SG1 2NY, Stevenage, UK

Abstract

A deconstruction of previously reported PI3K δ inhibitors and subsequent regrowth led to the identification of a privileged fragment for PI3K δ which was exploited to deliver a potent, efficient and selective lead series with a novel binding mode observed in the PI3K δ crystal structure.

Introduction

Phosphoinositide 3-kinase δ (PI3K δ) and the closely related isoforms PI3K α , β and γ are class I lipid kinases, which catalyse the phosphorylation of phosphatidylinositol 4,5-bisphosphate to produce the key signalling molecule phosphatidylinositol 3,4,5-triphosphate, which in turn triggers a series of downstream biological events that affect cell growth, chemotaxis, differentiation, proliferation and survival¹⁻⁵. The PI3K α and β isoforms are ubiquitously expressed in all tissues and knock-out mice are embryonically lethal, whereas PI3K δ and γ are predominantly expressed in leukocytes and mutagenic mice are viable with a phenotype consistent with immunological effects on B-cells, T-cells, and neutrophils, making them a target for the treatment of inflammatory conditions, such as asthma and COPD⁶⁻⁸. Many selective PI3K δ inhibitors have been reported⁹⁻¹⁰, predominantly for oncology indications (for example Idelalisib¹¹ (fig. 1.)), although AM-8508 (fig. 1) was reported by Amgen as a potential treatment for inflammatory diseases¹², leniolisib was progressed by Novartis into phase III trials for the treatment of activated PI3K delta syndrome¹³ and UCB have progressed seletalisib into clinical trials for patients with primary Sjogren's syndrome¹⁴. We previously reported¹⁵ the discovery of highly potent PI3K δ inhibitors nemiralisib, **1** and GSK2292767, **2** (fig. 1) for the treatment of respiratory indications via inhalation. Both these compounds are highly selective for PI3K δ (≥ 1000 -fold) with ideal properties for inhaled delivery (low bioavailability and moderate to high clearance) and are progressing through clinical trials¹⁶⁻¹⁹. In this

communication, we describe the successful discovery of selective leads for PI3K δ with different chemical starting points compared to inhaled clinical compounds **1** and **2**, achieved via a deconstruction and regrowth approach.

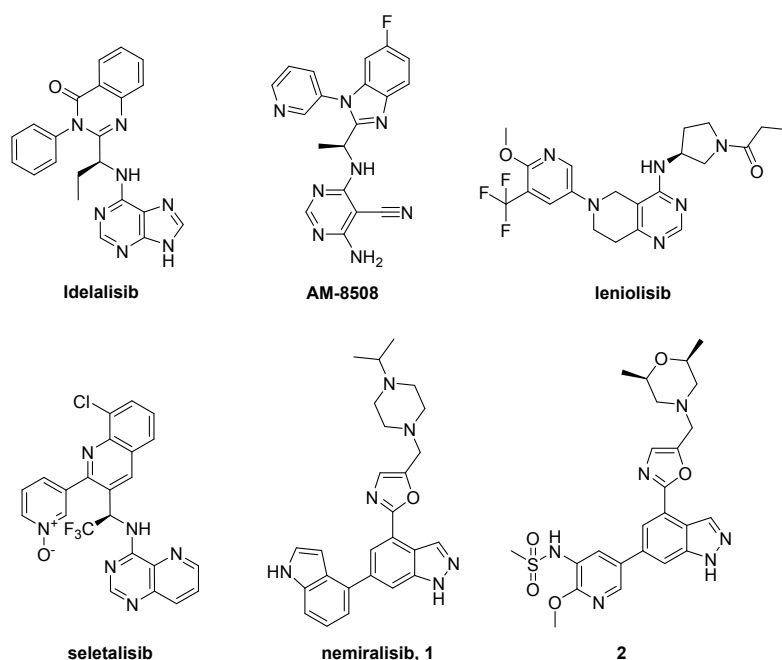


Figure 1. Selected PI3K δ inhibitors.

Results and Discussion

We recently reported a lead series developed from an initial small, focussed array²⁰ and herein we describe a broader approach leading to the discovery of a further lead series. A key focus in this exploration was to identify PI3K isoform selectivity differences such that subsequent lead optimisation studies would be better placed to deliver highly selective compounds.

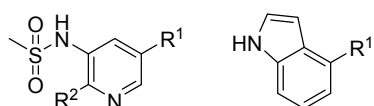
The binding modes of compounds **1** and **2**, which had been determined based on homology modelling and later confirmed by crystallography¹⁵, indicated that the indole/pyridine sulfonamide group occupied the affinity pocket region of the kinase, the indazole made the key interaction with the “hinge” region and the oxazole/alkyl amine group accessed a region of the kinase known to impart selectivity for PI3K δ over the other isoforms²¹. A deconstruction of compounds **1** and **2** to compounds **3-5** (Table 1) was performed to enable better understanding of the minimum pharmacophore required for potency. The oxadiazole in compound **5** was chosen in place of the oxazole primarily for ease of synthesis and, with a pendant morpholine substituent, was previously shown to have no impact on PI3K potency¹⁵.

pIC ₅₀					
Compound Number	Structure	PI3Kδ (LE)	PI3Kα	PI3Kβ	PI3Kγ
1		9.9*	5.3 ^{ab}	5.8 ^a	5.2 ^c
2		10.1*	6.4	5.6	6.5
3		5.1 (0.39)	<3.8	4.6 ^c	<3.8
4		6.0 ^a (0.37)	5.1	5.1	5.6
5		3.8 ^d (0.25)	<4.3	<4.3	4.6 ^a
6		6.4 (0.42)	5.2	5.4	5.6

Table 1. Inhaled clinical compounds **1** and **2** (data taken from reference¹⁵), deconstructed indazole compounds **3-5** and compound **6**. n ≥ 3. *pKi reported from the standard assay ran at a 2 mM ATP concentration. a: Tested pIC₅₀ < 4.6 on one occasion. b: Tested <5.3 on one occasion. c: Tested pIC₅₀ <4.6 on three occasions. d: n=1, tested at high concentration to determine a pIC₅₀.

Compound **3** was an efficient fragment compound; however, it was approximately 10-fold less potent than compound **4**. We proceeded to synthesise a representative fragment that we anticipated would engage the PI3K δ selectivity region of the protein²¹, however compound **5** was inactive in our assay when tested at standard concentrations, highlighting the importance of occupying the lipid kinase affinity pocket to enable measurement of the activity of suitable fragments. This led us to also synthesise the 2-chloro substituent on the pyridine, compound **6**, due to our previous observation that a 2-chloro substituent displayed enhanced potency over the 2-methoxypyridine substituent in the primary enzyme assay. This proved to be the case for the fragments herein such that compound **6** was more potent and efficient than compound **4**.

With this data in hand we planned to construct a compound set (Fig. 2) that enabled exploration of the hinge binder from either 2-chloro and 2-methoxy pyridines or an indole, with the aim of identifying novel, PI3K δ -selective hinge binders at R¹.



R² = Cl, OMe

Figure 2. Outline structures of planned array.

To design and select hinge binders a two-stepped approach was adopted. Firstly, an open-minded, inclusive approach was taken to identify novel putative hinge binding groups, as our hypothesis was that PI3K isoforms demonstrated a wider tolerance for hinge binding groups in the ATP binding site compared to many protein kinases. In addition to accommodating hinge binding groups with only an H-bond acceptor, a tolerance for saturated and therefore more bulky hinge binding groups (morpholine, for example) was reported²². This was believed to be a critical advantage for maximising protein kinase selectivity of lipid kinase-targeted compounds.

Secondly, a modelling approach was applied to help evaluate and prioritise for synthesis the list of proposed hinge binders, and in order to develop a fuller understanding of the potential interaction features of these moieties, the Cresset field based representation was applied²³. A 3D molecular interaction potential (MIP) built from an extended atom forcefield was used to generate a more detailed model of the electrostatics that better described the projected interactions of the template than traditional point charge models. In this case a crystal structure pose of compound **3** in PI3K δ was used as a template from a representative crystal structure and the designed hinge binder

fragments attached to the indole group were aligned to this template pose guided by the MIPs in the Cresset software.

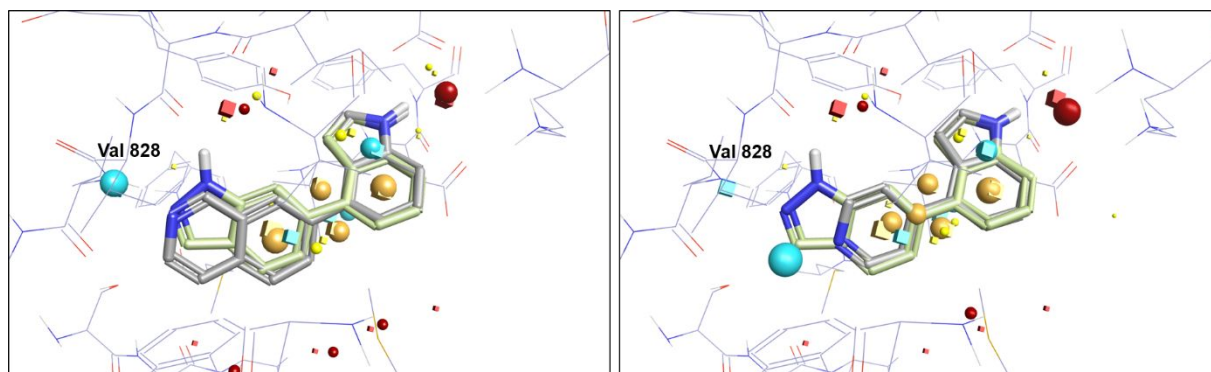


Figure 3. Cresset field point features of an indole affinity pocket group with either an isoquinoline hinge binder (left) or a pyridine hinge binder (right) overlaid with template compound **3**. Field points for the template and query molecules are represented as cubes and spheres, respectively. Field point colors denote donor (red), acceptor (blue), hydrophobic minima (gold) or shape (yellow) features and size indicates the magnitude of the feature.

As an example, an isoquinoline hinge binder (fig. 3, left) fitted the features of the indazole template very well, with the field point features of the quinoline (spheres) closely matching the features of the template (cubes). Moreover, it was apparent that the H-bond acceptor feature of the hinge binder fitted nicely against the Val828 backbone H-bond donor of the kinase hinge residue, although this was not used to drive the overlay. By contrast, the overlay of the pyridyl hinge binder (fig. 3b) with the indazole template was very poor and the H-bond acceptor feature of the pyridine nitrogen was not accessible to the kinase hinge region without disrupting the overlay of the indole moiety. The same approach was taken for the pyridine sulfonamide and a similar outcome was observed. To test the applicability of using the Cresset approach to rank compounds for synthesis, an initial set of compounds was selected and synthesised, including hinge binders predicted to either fit well or fit poorly.

Data from this initial array demonstrated a large disconnect between the indole and the pyridine sulfonamide groups such that the pyridine sulfonamide group was substantially more accommodating to different hinge binders when compared to the indole, as exemplified by the compounds in Table 2. Compound **7** was approximately 400-fold more potent at PI3K δ than the indole equivalent compound **8** and substantially more ligand efficient (cf. a 25-fold change between compounds **9** and **10**). Since compounds **7** and **9** were equipotent, this further demonstrated the efficiency of the shorter hinge binder. In fact, as the PI3K enzyme assay floor was a pIC_{50} of 4.3 – 4.6 when operating at standard compound concentrations, the potency of certain indole compounds, for

example compound **8**, had to be determined using higher compound concentrations. From these data, we hypothesised that the pyridine sulfonamide was a privileged fragment specifically for PI3K δ , as the potency against PI3K α , β and γ was consistently lower for compounds **4**, **6**, **7** and **9**. Furthermore compound **7** was essentially inactive ($\text{pIC}_{50} < 5$) against a cross panel of 16 kinases screened (see supporting information).

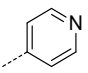
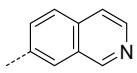
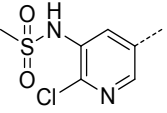
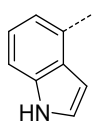
Compound Number pIC_{50} PI3Kδ , α , β and γ PI3Kδ LE	Hinge Binder	
		
	7 6.6 , 5.2, 6.1, 5.4 0.5	9 6.8 , 5.6, 5.6, 6.1 0.42
	8 4.1^{ab} , <4.3, <4.3, <4.3 0.37	10 5.4 , <4.5, 4.8, 4.8 ^c 0.39

Table 2. Selected compounds from the initial hinge binder array. $n \geq 3$. a: Tested at high concentration to determine a pIC_{50} . b: $n=2$. c: Tested $\text{pIC}_{50} < 4.6$ on one occasion.

These data validated the Cresset model for the indole group, demonstrating that the isoquinoline was indeed a more effective hinge binder than the pyridine but clearly demonstrated that the approach could not be applied to prioritise hinge binders for the pyridine sulfonamide. Furthermore, the data for the pyridine sulfonamide built confidence in the hypothesis that we had discovered a privileged fragment for PI3K δ inhibition that not only gave very potent and ligand efficient compounds, but also demonstrated reasonable selectivity over the other PI3K isoforms. To explore the potency and selectivity of the template in a more robust manner, we expanded the planned compound set to include variations to the *ortho*-pyridine and sulfonamide substituents. To enable synthesis of a manageable compound set and consistency when analysing the data generated, we chose to fix specific R-groups, when exploring the other R groups (fig. 4). The R^1 group was fixed as dihydropyran or an *N*-methylpyrazole, with R^2 as either chloro or methoxy to explore the R^3 sulfonamide substituents in more detail (fig. 4). Similarly, the R^3 sulfonamide was fixed as methyl or phenyl when exploring R^1 or R^2 further. The majority of compounds were synthesised from readily available sources via array chemistry, whilst the remainder were synthesised bespoke as necessary.

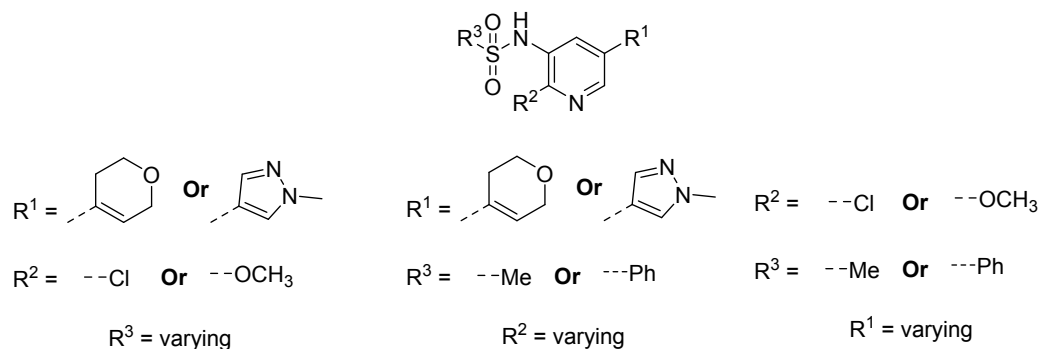


Figure 4. Compound set design to evaluate R^1 , R^2 and R^3 .

Once all the data was in hand and after determining that the data set had reasonable cross coverage (see supporting information, Fig. 1S), an R-group decomposition on the total 324 compounds synthesised was carried out (using the R-groups as defined in fig. 4), followed by a Free-Wilson analysis²⁴ applied to the potency data on each of the PI3K isoforms. The Free-Wilson prediction demonstrated a good correlation for all PI3K isoforms (see supporting information, Fig. 2S, 3S, 4S and 5S). This enabled evaluation of the contribution to PI3K isoform potency of each of the R-groups independently and by considering the different impact across all four PI3K isoforms, allowed a detailed assessment of the selectivity conferred by each R-group. The Free-Wilson analysis also provided a potency contribution from the core. For this data set, compounds were generally more potent at PI3K δ than the other isoforms, and this was reflected in the contribution of the core to the potency for the four isoforms (pIC_{50} 6.0, 5.2, 5.3 and 5.1 for PI3K δ , α , β and γ , respectively), further supporting our hypothesis that the pyridine sulfonamide was a privileged fragment for PI3K δ .

In figures 5, 6 and 7, selected R-groups (for which the structure is indicated by the index-linked tables 3, 4 and 5) are displayed on the x-axis and the average potency contributions to each isoform across the data set, as determined by the Free-Wilson analysis, are displayed on the y-axis, indicated by colored diamonds (PI3K δ in green, PI3K α in orange, PI3K β in red and PI3K γ in yellow). All compounds were evaluated in the production PI3K assay format, so the assay floor was $\text{pIC}_{50} \sim 4.6$ for all PI3K isoforms, and this was important to keep in mind when analysing selectivity differences between compounds of low potency. For instance, the core potency contribution was higher for PI3K δ , therefore R-groups for PI3K δ had a larger potential magnitude of negative potency contribution from the Free-Wilson analysis than the same R-groups for other PI3K isoforms.

A wide range of potency contributions were observed for the different hinge binders (R^1) across the different PI3K isoforms, despite the very high protein homology of the amino acid sequence in this region of the PI3K family

(fig. 5, table 3). Dihydropyran (R¹A) was moderately beneficial for all PI3K isoforms with some selectivity preference for PI3K δ . Tetrahydropyran (R¹B) lowered potency against all PI3K isoforms, demonstrating that there is a requirement for planarity in the immediate vicinity of the pyridine sulfonamide. *N*-linked morpholine (R¹C) demonstrated a small potency increase for PI3K δ and β , but to a lower extent than dihydropyran (R¹A), with some selectivity over PI3K α and γ . Homo-morpholine (R¹D) was tolerated by all isoforms except PI3K γ . Racemic 2-methylmorpholine (R¹E) increased potency and selectivity in a comparable manner to dihydropyran (R¹A) and was substantially better than racemic 3-methylmorpholine (R¹F). 2-Oxa-6-azaspiro[3.3]heptane (R¹G) and racemic 2,6-dimethylmorpholine (R¹H) were essentially inactive at all PI3K isoforms, further demonstrating the requirement for some planarity in the region adjacent to the pyridine ring and the lack of space for di-substitution on the morpholine. 2-Ethylmorpholine (R¹I) was tolerated for all isoforms but preferentially increased potency at PI3K α and γ . Most of the more differentiated potential hinge binders, such as, thiomorpholine 1,1-dioxide (R¹J) and cyclohex-2-enone (R¹K) were also essentially inactive against all PI3K isoforms. *N*-methylpyrazole (R¹L) and pyrazole (R¹M) were both tolerated reasonably well by all isoforms when linked in the 4-position and *N*-methylimidazole (R¹N), linked in the 5-position, was tolerated by all PI3K isoforms except PI3K γ . Pyrazole (R¹O), linked in the 3-position, was less potent against all PI3K isoforms. Surprisingly, incorporation of a phenyl “hinge binder” (R¹P) was tolerated with only a small reduction in potency at all PI3K isoforms. This observation highlights the exceptional tolerance that the PI3K isoforms can have to different hinge binders if a preferred affinity pocket group is appropriately situated. Pyridine (R¹Q), substituted in the 4-position gave a small boost to PI3K δ and β over PI3K α and γ , whereas 3-substituted pyridine (R¹R) was tolerated equally by all isoforms with only a small potency reduction. 4-Substituted 2-methylpyridine (R¹S) was tolerated for all isoforms, with a slight bias for PI3K α . Thiazole (R¹T) boosted PI3K δ potency more than the other isoforms and isothiazole (R¹U) showed the same profile, albeit at a lower overall potency increase. 5-Substituted pyrimidine (R¹V) increased PI3K δ a small amount whilst not affecting the other isoforms. 4-Substituted 2-aminopyrimidine (R¹W) showed a large preference for PI3K γ over the other isoforms but one of the more dramatic discoveries was the 5-substituted 2-aminopyrimidine (R¹X) which, while demonstrating increased potency at all isoforms, had a very strong preference for PI3K γ . Removing a nitrogen from R¹X to give 5-substituted 2-aminopyridine (R¹Y) was tolerated but much less beneficial for all the PI3K isoforms. Aryl ethers were also tolerated as hinge binders, for example 3-methoxyphenyl (R¹Z) was tolerated by all PI3K isoforms and 4-methoxyphenyl (R¹ZA) boosted PI3K α and γ much more than PI3K δ and β . Aryl carboxamides and sulfonamides (such as R¹ZB and R¹ZC) were not well tolerated by any PI3K isoform. Other hinge binders that were tolerated include 3-fluoro-4-chlorophenyl (R¹ZD)

and 3-fluoro-4-hydroxyphenyl (R¹ZE) although both had a slight preference for PI3K γ . Following on from this thorough exploration of R¹ we identified the dihydropyran (R¹A) and morpholine (R¹C) groups as giving the best balance of potency increase and selectivity for PI3K δ over the PI3K isoforms, whilst keeping the aromatic ring count low.

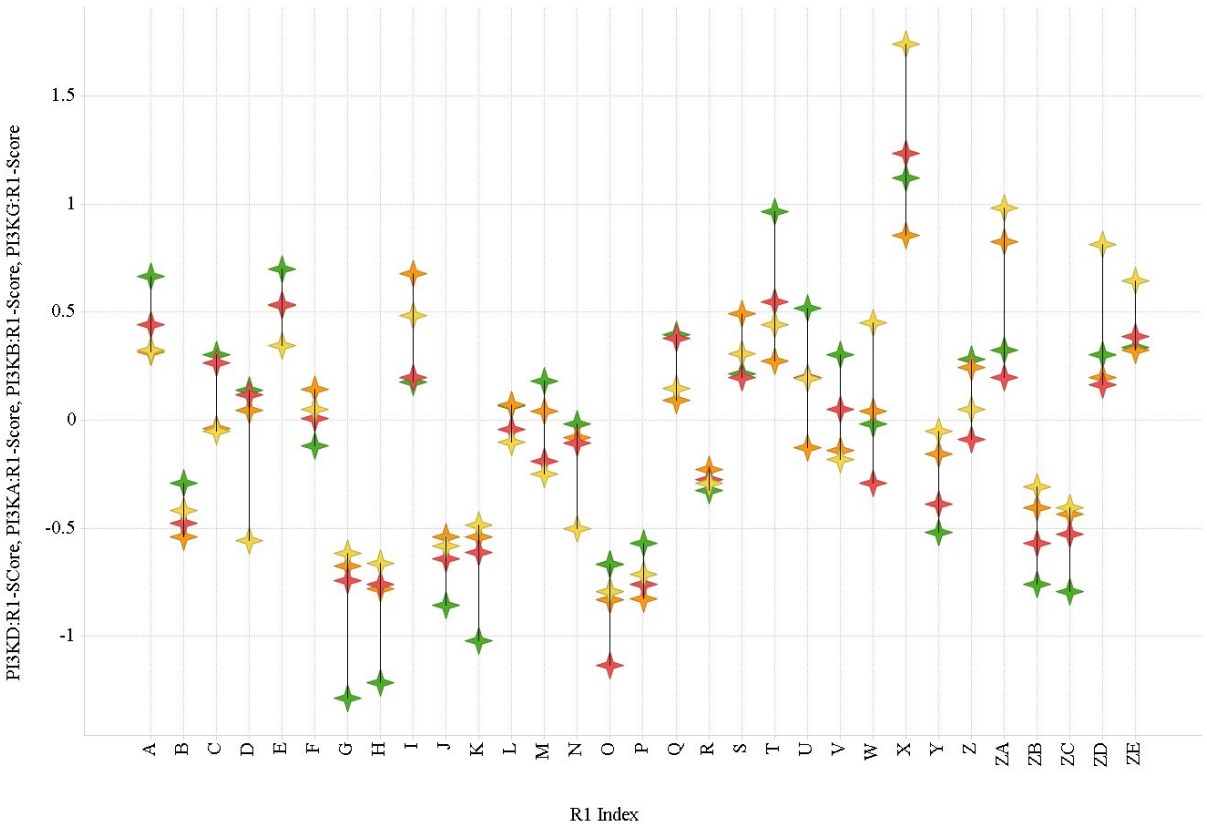


Figure 5. A representative set of R¹ group contribution scores to PI3K δ , α , β and γ potency (green, orange, red and yellow, respectively), normalised to R¹L.

A		B		C		D		E		F	
G		H		I		J		K		L	
M		N		O		P		Q		R	
S		T		U		V		W		X	
Y		Z		ZA		ZB		ZC		ZD	
ZE											

Table 3: Structures of the representative set of R^1 groups. R^1 groups highlighted by * are based on one compound.

All other data was derived from two or more compounds.

Focussing on the R^2 substituent (fig. 6, Table 4), the methoxy (R^2A) and chloro (R^2B) substituents confirmed our original observations that the chloro was generally higher potency than methoxy across all PI3K isoforms, with little preference for PI3K δ . A trifluoromethyl substituent (R^2C) boosted potency further at all PI3K isoforms other than PI3K γ , indicating the preference for an electron withdrawing group at this position. However, the cyano substituent (R^2D) only showed similar potency to the methoxy group at PI3K δ and β and was less potent at PI3K α and γ indicating that some lipophilicity was required or that the H-bond acceptor of the cyano group is less tolerated in those isoforms. The difluoromethoxy substituent (R^2E) had similar potency to the cyano for PI3K δ and β but was less potent at PI3K α and γ . This substituent, along with the cyano, therefore would provide a good option to enhance selectivity of PI3K δ over PI3K α and γ if that were required during later lead optimisation studies. Extending the methoxy group to ethoxy (R^2F) reduced all PI3K isoform activity marginally and the

trifluoroethoxy substituent (R^2G) was significantly worse. Replacement of the substituent with hydrogen (R^2H) had a significant impact on PI3K δ potency and lowered potency at PI3K α , β and γ . Changing to a methyl substituent (R^2I) was also detrimental to potency for all PI3K isoforms albeit more tolerated in PI3K δ . An isopropyl substituent (R^2J) reduced potency at all PI3K isoforms and the methylamino substituent (R^2K) was similarly detrimental. Finally, the hydroxyl substituent (R^2L) was also lower potency for all PI3K isoforms, potentially due to the propensity for hydroxy pyridines to prefer the pyridone tautomer²⁵ which is not tolerated in this region of the PI3K isoforms. After this exploration of R^2 groups, the methoxy (R^2A) and chlorine (R^2B) remained our preferred R^2 groups for their PI3K δ . We considered the trifluoromethyl (R^1C) group as interesting SAR but too lipophilic for further consideration.

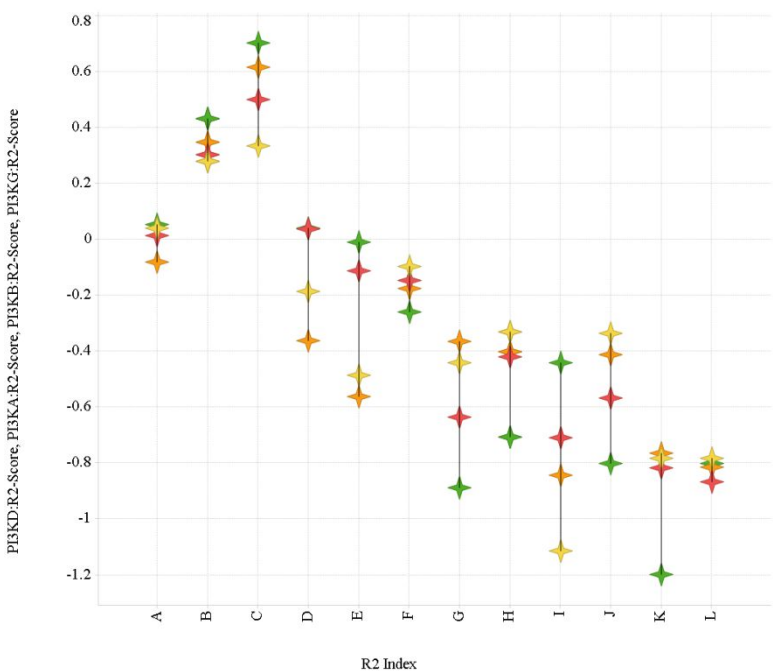


Figure 6. Representative set of R^2 group contribution scores to PI3K δ , α , β and γ potency (green, orange, red and yellow, respectively), normalised to R^2A .

A 	B 	C 	D 	E 	F
G 	H 	I 	J 	K 	L

Table 4. Structures of the representative set of R^2 groups. All R^2 group data was derived from two or more compounds.

Finally, consideration of the sulfonamide substituent, R^3 , revealed some unexpected SAR (fig. 7, Table 5). Firstly, alkyl groups, such as methyl (R^3A), were generally less potent than phenyl (R^3B) for all PI3K isoforms. Similarly, a cyclohexyl group (R^3C) was not well tolerated and potency was lower for all PI3K isoforms. 4-Cyanophenyl (R^3D) increased the potency for PI3K α but not for the other isoforms, whereas 4-hydroxyphenyl (R^3E) was more potent against all isoforms. 4-Methoxyphenyl (R^3F) was not substantially different to phenyl (R^3B). The 3-cyanophenyl group (R^3G) was more potent for all PI3K isoforms and especially so for PI3K δ and β . The 3-methoxyphenyl (R^3H), 2-methylphenyl (R^3I) and 3-pyridyl (R^3J) groups all increased potency for all PI3K isoforms to a similar level above the phenyl (R^3B). Different heterocycles were generally well tolerated, for example an imidazole group (R^3K) boosted PI3K δ and β without increasing PI3K α and γ . A thiazole group (R^3L) increased potency at all isoforms, with a preference for PI3K β , whereas a phenylthiazole group (R^3M) increased potency at all isoforms, with a dramatic preference for PI3K δ , especially over PI3K β . A benzylimidazole group (R^3N) also selectively increased PI3K δ potency whilst having much less impact on the other isoforms. A benzyl group (R^3O) showed similar potency to the phenyl (R^3B). Finally, initial attempts to reach the selectivity pocket using groups with a dimethyl morpholine (R^3P or R^3Q) were not successful and lowered potency against all PI3K isoforms. After this exploration, we were left with a selection of interesting R^3 groups and a clear indication that this was a suitable position on the template to explore further, with scope to modulate potency, selectivity and physicochemical properties.

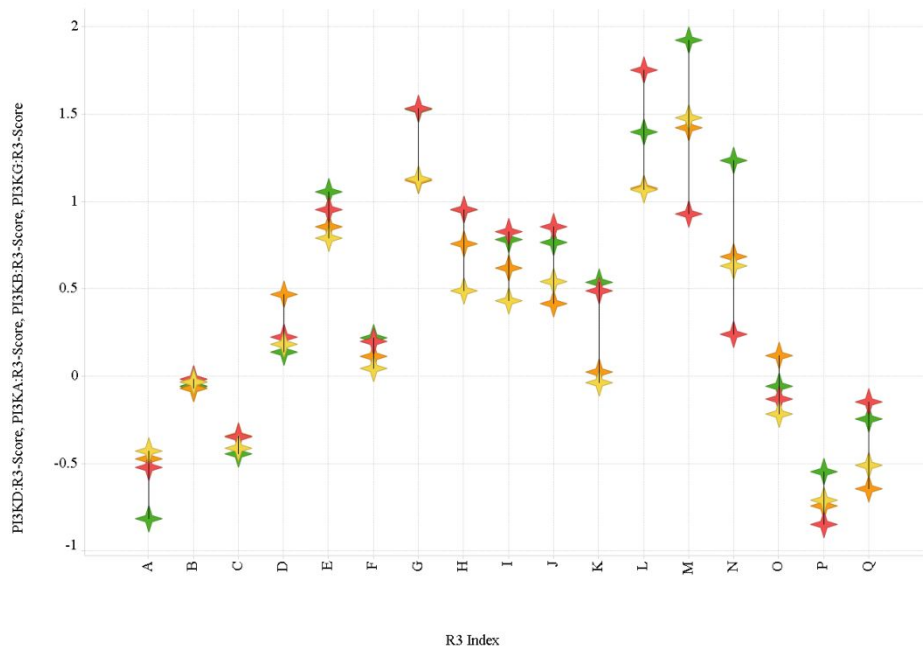


Figure 7. Representative set of R³ group contribution scores to PI3K δ , α , β and γ potency (green, orange, red and yellow, respectively), normalised to R³B.

A 	B 	C 	D 	E 	F
G 	H 	I 	J 	K 	L
M 	N 	O 	P 	Q 	

Table 5. Structures of the representative set of R³ groups. R³ groups highlighted by * are based on one compound.

All others R³ groups were derived from two or more compounds.

The following compounds from the synthesised compound set (Table 6) were selected to highlight the trends observed. Compound **11** was amongst the most efficient compounds with an LE for PI3K δ of 0.53 and reasonable PI3K isoform selectivity. For compound **12** the PI3K γ activity increased more than 10-fold compared to compound **11**, whilst the other PI3K isoforms all increased less than 3-fold, demonstrating that even with a hinge binder that demonstrated a clear selectivity preference for PI3K γ , the pyridine sulfonamide resulted in a compound that was equipotent at PI3K δ and PI3K γ . Compound **13** demonstrated the increase in PI3K enzyme potency obtained when changing a methyl group to a phenyl across all PI3K isoforms, although the LE was slightly lower than for compound **11**. Compound **14** contained a phenyl hinge binder and, although the potency for PI3K δ was 100-fold lower than compound **13**, clearly demonstrated the broad tolerance for short, flat hinge binders attached to the pyridine sulfonamide template. The difference between the methoxy and chlorine R² group was exemplified by compound **15** which is a less potent and efficient PI3K δ inhibitor than compound **13**, but maintains equivalent PI3K isoform selectivity. Compound **16** was an example of the most PI3K isoform selective compound made in this compound set, with ≥ 100 -fold selectivity for PI3K δ over the PI3K isoforms. This selectivity came at the price of ligand efficiency (LE = 0.36), inferring that, although this R³ group may not offer much additional potency for PI3K δ over other R³ groups, it reduced relative potency at the other PI3K isoforms. Compound **16** was also ≥ 100 -fold selective against a cross-panel of 29 kinases (see supporting information) and inactive in a hERG binding assay ($\text{pIC}_{50} < 4.3$). Compound **16** had a pIC_{50} of 7.3 in a peripheral blood mononuclear cell assay, using Cytostim to stimulate interferon γ production from the T-lymphocyte compartment¹⁵. Passive permeability on MDCK cells

for compound **16** was high (466 nm/sec) and CLND solubility was 12 µg/mL. Protein binding (human serum albumin) was 89.9% and microsomal clearance was high in rat and human, 17.4 and 7.9 mL/min/g, respectively.

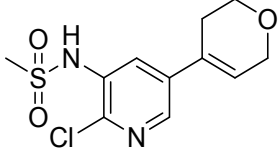
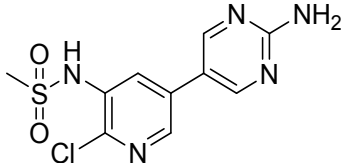

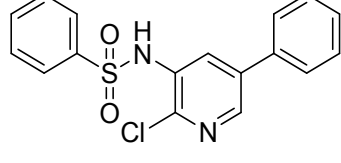
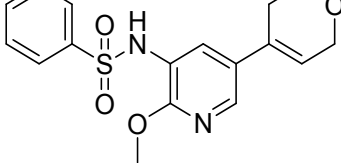
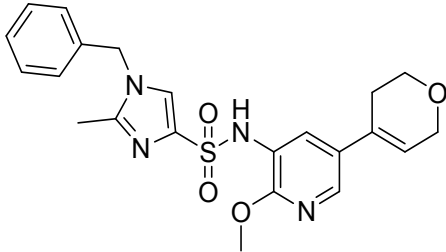
Compound Number	Structure	pIC ₅₀			
		PI3Kδ (LE)	PI3Kα	PI3Kβ	PI3Kγ
11		6.9 (0.53)	5.6	6.3	5.5
12		6.9 (0.5)	5.8	6.8	6.7
13		8.0 (0.48)	6.3	6.9	6.3
14		6.0 (0.36)	4.5	4.8	4.9 ^a
15		7.4 (0.42)	5.7	6.4	5.9
16		8.2 (0.36)	6.2	6.0	6.0

Table 6: Specific compounds from the synthesised compound set. n ≥ 3. a: Tested pIC₅₀ < 4.6 on two occasions.

To try and understand the origins of the selectivity and efficiency of the series, a crystal structure of compound **11** was obtained in PI3Kδ (as previously described²⁶) (fig. 8). The dihydropyran oxygen made the anticipated

acceptor interaction with Val828 in the hinge-region of the kinase and maintained planarity in the region of the pyridine ring, providing further evidence for the low potency of those hinge binders with more 3-dimensional structure in the region (e.g. tetrahydropyran, R¹B). The pyridine nitrogen made an H-bond interaction to stabilise a crystallographically observed water, bridging to Asp787 and Tyr813, and the sulfonamide group made a bridging interaction between Lys779 and Trp760. This gave some insight into the preference for electron withdrawing substituents at R², which would increase the ionisation of the sulfonamide and thereby enhance the strength of the interaction with Typ760 and Lys779. This also implied that the pyridine nitrogen H-bond to water was not the key driver of potency. The crystal structure also indicated why bulkier R² groups were less potent due to the lack of space in the protein to accommodate them.

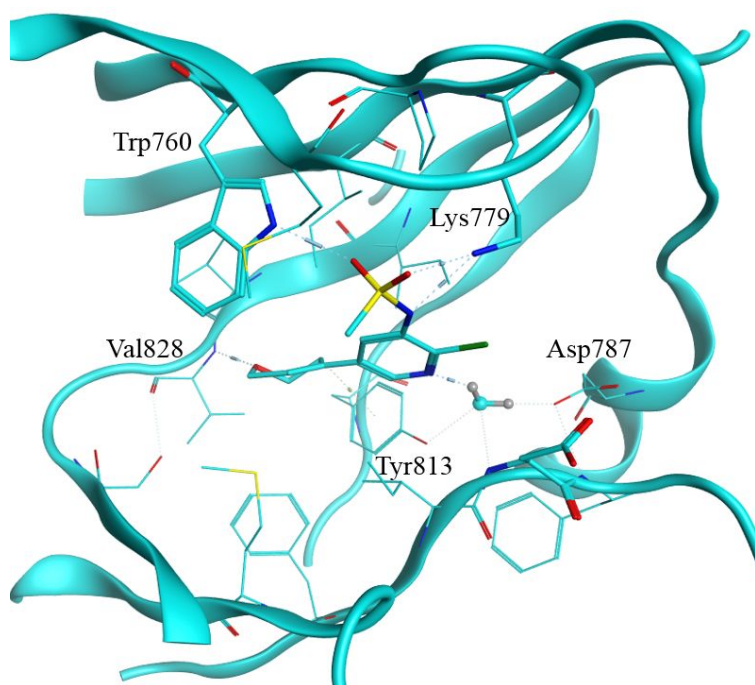


Figure 8. Compound **11** (cyan) crystal structure with PI3K δ .

Comparison of the PI3K δ crystal structure of compound **2**¹⁵ with compound **11** (fig. 9) showed distinct changes in the PI3K δ binding site. Firstly, the pyridine sulfonamide moiety of compound **11** was substantially closer to the hinge region due to the shorter dihydropyran hinge binder (this compound movement led us to adopt the name “Short hinge” for this series) and Lys779 moved to maintain the beneficial interaction with the sulfonamide group. Secondly, Trp760, with which compounds **1** and **2** interacted to gain significant PI3K δ selectivity, rotated through 180° in order to make the H-bond with an oxygen of the sulfonamide of compound **11**. We believed this additional interaction with Trp760 contributed to the enhanced potency and ligand efficiency observed for this short hinge

series when compared to the indazole series. The indole affinity pocket group of compound **8**, for example, was unable to make the same interactions and was therefore less potent and ligand efficient. The altered location of Trp760 may also explain why our initial attempts to obtain similar interactions to those observed with compounds **1** and **2** with groups such as R³P and R³Q were not successful. The water-mediated H-bond interaction from the nitrogen of the pyridine group to Asp787 and Tyr813 is observed for both compounds **2** and **11**, despite the significant ligand movement. Previously reported PI3K γ crystal structures of non-specific inhibitors of lipid kinases containing a pyridine sulfonamide, such as those reported by D'Angelo *et al.*²⁷, Nishimura *et al.*²⁸, and Knight *et al.*²⁹, demonstrated a similar binding mode to compound **2**.

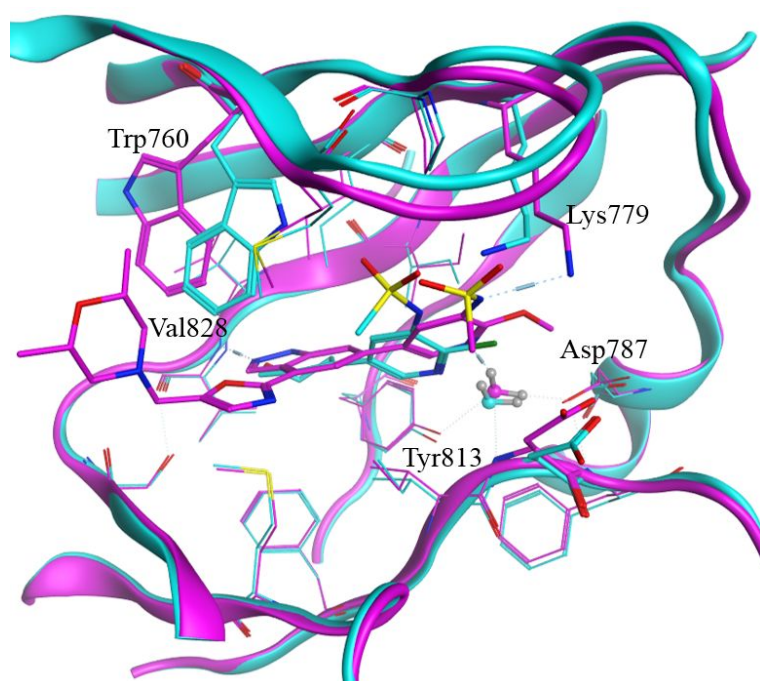


Figure 9. Compound **11** (cyan) PI3K δ crystal structure overlaid with compound **2** (purple).

We also obtained a crystal structure of compound **14** in PI3K δ which demonstrated an almost identical binding mode to compound **11** (fig. 10) with only a small movement away from the hinge region observed, presumably due to the lack of a strong H-bond between Val828 and the phenyl group 'hinge binder'. Compound **14** maintained the key H-bonds with Trp760 and Lys779, albeit with small positional differences and also maintained the through-water interactions with Tyr813 and Asp787. This non-differentiated binding mode once again demonstrated the broad tolerance of the privileged pyridine sulfonamide when attached to diverse hinge binders.

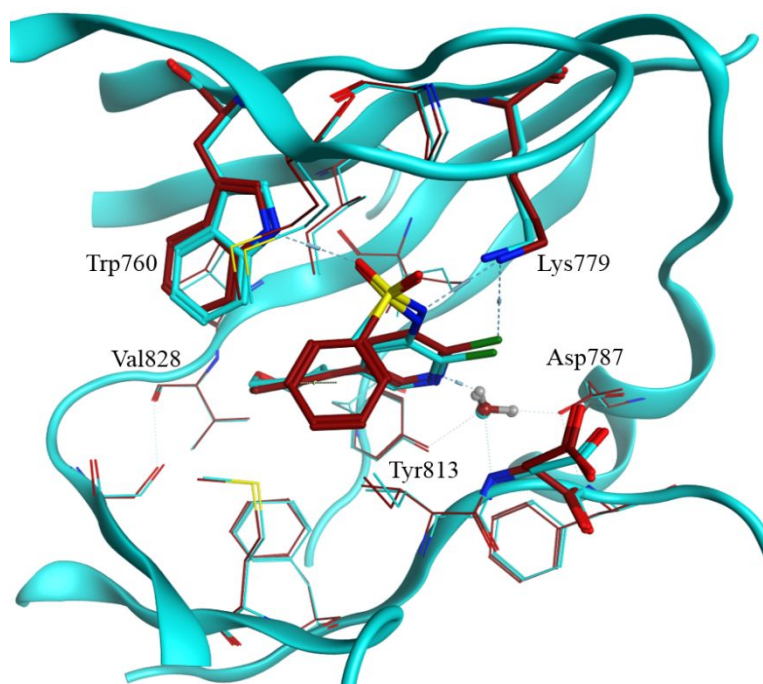


Figure 10. Compound **14** (maroon) PI3K δ crystal structure overlaid with compound **11** (cyan).

Finally, a crystal structure of compound **16** in PI3K δ was obtained and overlaid with compound **11** (fig. 11). This demonstrated that compound **16** made the same interactions with Val828, Trp760 and Lys779 as compound **11**, albeit with a slight rotation of the pyridine group, potentially to accommodate the longer R² methoxy group of compound **16** over the chlorine in compound **11**. The benzyl imidazole substituent of the R³ group occupied the ribose pocket, but was not close enough to make the same selectivity-enhancing interaction with Trp760 as compounds **1** and **2**. Furthermore there were no isoform residue differences between the PI3K isoforms in the immediate vicinity of this R³ group that could directly rationalise the observed selectivity. Other R³ groups that were able to occupy this space in PI3K δ (for example R³M) displayed enhanced selectivity over shorter substituents, indicating it as an interesting area to explore during subsequent lead optimization studies.

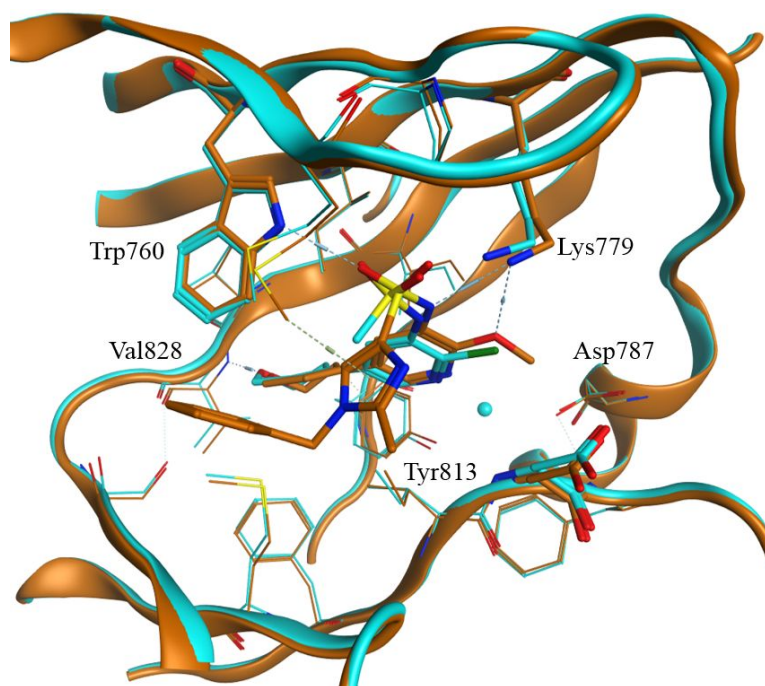


Figure 11. Compound **16** (gold) PI3K δ crystal structure overlaid with compound **11** (cyan).

Conclusions

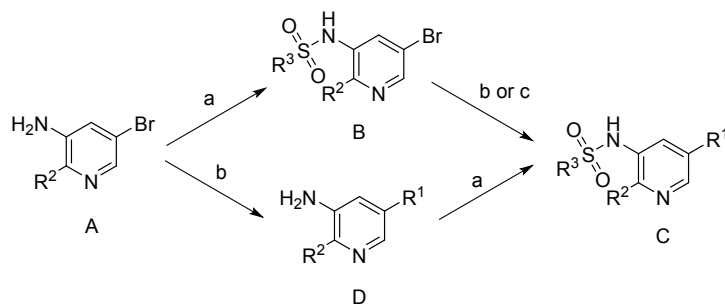
Through a deconstruction and regrowth of potent inhaled clinical compounds **1** and **2**, we have discovered and exploited a pyridine sulfonamide privileged fragment for PI3K δ that tolerated attachment to a broad range of hinge binders, including those that do not make a formal H-bond interaction with the hinge region of the PI3K isoforms, due to a novel binding mode observed in the PI3K δ crystal structure. Furthermore, we determined that different hinge binders attached to the pyridine sulfonamide can have a substantial effect on PI3K isoform potency and selectivity, even in a region of the protein known to be homologous across all PI3K isoforms. This moiety, in combination with certain hinge binders that showed a relative preference for different PI3K isoform, resulted in compounds equipotent at PI3K δ , further demonstrating that the pyridine sulfonamide is a privileged fragment for PI3K δ ; an observation that fitted well with known literature compounds containing a pyridine sulfonamide²⁷⁻²⁹ that were also equipotent across PI3K isoforms. Finally we reported compound **16**, a potent and selective inhibitor of PI3K δ , and an exemplar of a series suitable for further lead optimisation studies.

Experimental Section

Chemistry. General. All solvents and reagents, unless otherwise stated, were commercially available and were used as purchased without further purification. Proton and carbon nuclear magnetic resonance (^1H NMR and ^{13}C NMR) spectra were recorded on a Bruker AVI (400 MHz), Bruker Nano (400 MHz), Bruker DPX300 (300 MHz) or Bruker AVII+ (600 MHz) spectrometer (with cryoprobe) in the indicated solvent. Chemical shifts δ are reported in parts per million (ppm) relative to tetramethylsilane and are internally referenced to the residual solvent peak. HRMS data were recorded on a Waters XEVO G2-XS QToF. Coupling constants (J) are given in hertz (Hz) to the nearest 0.1 Hz. LCMS and HPLC methods are detailed in the Supporting Information. The purity of all compounds screened in the biological assays was examined by LCMS analysis and was found to be $\geq 95\%$ unless otherwise specified. Mass directed automated preparative HPLC (MDAP) methods are detailed in the Supporting Information.

Compounds were generally synthesised as described in Scheme 1. Reacting amine **A** with R^3 -sulfonyl chlorides gave aryl bromides **B**, which could be subjected to Suzuki-Miyaura cross-coupling with a boronic acid or ester, or alternatively subjected to Buchwald-Hartwig cross-coupling with an amine, to give target compounds **C**.

These steps could be reversed, giving intermediates amines **D**, to vary the sulfonamide group.



Scheme 1. Synthesis of array compounds. (a) $\text{R}^3\text{-SO}_2\text{Cl}$, in pyridine or THF with DIPEA; (b) R^1 -boronic acid or ester, Pd catalyst ($\text{Pd}(\text{dppf})\text{Cl}_2$, $\text{Pd}(\text{PPh}_3)_4$, or chloro(di-2-norbornylphosphino)(2'-dimethylamino-1,1'-biphenyl-2-yl)palladium(II)), base (Na_2CO_3 , K_2CO_3 or K_3PO_4), solvent (1:4-dioxane or THF, in water); (c) amine, $\text{Pd}_2(\text{dba})_3$, Cs_2CO_3 , RuPhos, DMF:1,4-dioxane.

Exemplified compounds were synthesised as follows:

6-(1H-Indol-4-yl)-1H-indazole, 3. 6-Bromo-1H-indazole (100 mg, 0.51 mmol), sodium carbonate (161 mg, 1.52 mmol) and PdCl_2dppf (37.1 mg, 0.051 mmol) were added to a microwave vial. 1H-Indol-4-ylboronic acid (90 mg,

0.558 mmol) was dissolved in 1,4-dioxane (8 mL) and added to the vial followed by water (2 mL). The reaction was heated to 80 °C for a total of 3 h. The residue was separated between DCM (20 mL) and brine (20 mL), the organic layer was evaporated to dryness and the mixture was purified using MDAP (method A). Pure fractions were combined and evaporated under a stream of nitrogen to give the title compound, 29.5 mg (25% yield). LCMS (method A): 100%, $r_t = 0.91$, $[M+H]^+ = 234$. 1H NMR (400 MHz, DMSO- d_6) δ_H 13.08 (br s, 1H), 11.29 (br, s, 1H), 8.33 (HCOOH, 10% by weight), 8.11 (s, 1H), 7.86 (d, $J=8.6$ Hz, 1H), 7.75 (m, 1H), 7.44 (m, 3H), 7.21 (t, $J=7.8$ Hz, 1H), 7.16 (dd, $J=7.3$, 0.8 Hz, 1H), 6.59 (br, s, 1H). HRMS (ESI) for $C_{15}H_{12}N_3$ $[M+H]^+$ calcd.: 234.1032, found: 234.1039.

***N*-(5-(1*H*-Indazol-6-yl)-2-methoxypyridin-3-yl)methanesulfonamide, 4.** See compound 4 in ref ²⁰.

4-[5-(4-Morpholinylmethyl)-1,3,4-oxadiazol-2-yl]-1*H*-indazole, 5. 6-Bromo-4-[5-(4-morpholinylmethyl)-1,3,4-oxadiazol-2-yl]-1-(phenylsulfonyl)-1*H*-indazole (compound **S4**, 500 mg, 0.991 mmol) was dissolved in ethyl acetate (60 mL) and added to Palladium on carbon (158 mg, 0.149 mmol) and left under hydrogen for 2 days. The reaction mixture was filtered through Celite and the solvent removed *in vacuo*. The residue was dissolved in isopropanol (10 mL) and 2M sodium hydroxide (aq.) (0.992 mL) and stirred overnight. The reaction mixture was diluted with water (10 mL) and extracted with DCM (2 x 10 mL). The organic layer was passed through a hydrophobic frit and concentrated *in vacuo*. The residue was purified by silica chromatography (50 g column) eluting with 0 - 100% ethyl acetate in cyclohexane over 40 min, followed by 100% methanol. The methanol fractions were purified by silica chromatography (50 g) eluting with 0 - 15% methanol (containing 1% triethylamine) in DCM over 40 min. Product containing fractions were purified by silica chromatography (50 g) eluting with 0 - 25% methanol in DCM over 60 min. Pure fractions were combined and dried to give title compound, 80 mg (28% yield). LCMS (method A): 93%, $r_t = 0.52$, $[M+H]^+ = 286$. 1H NMR (400 MHz, DMSO- d_6) δ_H 13.55 (br. s., 1H), 8.54 (s, 1H), 7.77-7.87 (m, 2H), 7.54 (t, $J=7.9$ Hz, 1H), 3.96 (s, 2H), 3.61 (t, $J=4.8$ Hz, 4H), 2.54 (t, $J=4.8$ Hz, 4H). HRMS (ESI) for $C_{14}H_{16}N_5O_2$ $[M+H]^+$ calcd.: 286.1305, found: 286.1308.

***N*-[2-Chloro-5-(1*H*-indazol-6-yl)-3-pyridinyl]methanesulfonamide, 6.** 6-(4,4,5,5-Tetramethyl-1,3,2-dioxaborolan-2-yl)-1*H*-indazole (100 mg, 0.41 mmol), *N*-(5-bromo-2-chloropyridin-3-yl)methanesulfonamide¹⁵ (117 mg, 0.410 mmol), and tetrakis(triphenylphosphine) palladium (0) (23.7 mg, 0.02 mmol) were weighed to a microwave vial. The vial was sealed and THF (3 mL) was added followed by potassium carbonate (56.6 mg, 0.41 mmol) in water (2 mL). The reaction was heated at 150 °C for 2 h. The reaction was diluted with DCM (30 mL) and washed with brine (30 mL) and water (2 x 30 mL). The organic layer was passed through a hydrophobic frit

and concentrated under vacuum. The aqueous layer was concentrated under vacuum. Both residues were purified by MDAP (method A). Product fractions were combined and evaporated to dryness to give title compound, 25 mg (19% yield). LCMS (method A): 93%, $r_t = 0.73$, $[M+H]^+ = 323/325$. 1H NMR (400 MHz, DMSO- d_6) δ_H 13.28 (br. s., 1H), 10.00 (br. s., 1H), 8.62 (d, $J=2.5$ Hz, 1H), 8.11-8.18 (m, 2H), 7.91 (d, $J=8.6$ Hz, 1H), 7.84 (s, 1H), 7.46 (dd, $J=1.4, 8.4$ Hz, 1H), 3.17 (s, 3H). HRMS (ESI) for $C_{13}H_{12}ClN_4O_2S$ $[M+H]^+$ calcd.: 323.0370, found: 323.0371.

***N*-(6-Chloro-3,4'-bipyridin-5-yl)methanesulfonamide, 7.** A mixture of *N*-(5-bromo-2-chloropyridin-3-yl)methanesulfonamide (286 mg, 1 mmol), pyridin-4-ylboronic acid (246 mg, 2.000 mmol), Na_2CO_3 (318 mg, 3.00 mmol) and $PdCl_2dppf$.DCM (82 mg, 0.1 mmol) in 1,4-dioxane and water (10 mL, 4:1, v/v) under nitrogen was heated at 70 °C for 4 h, then filtered. The filtrate was concentrated and the residue was purified by silica chromatography (methanol: DCM, 1:50) to obtain a crude product. The crude was washed with ethyl acetate (5 mL), filtered and dried *in vacuo* to give the title compound 56 mg (20% yield). HPLC (method A): 99.5%, $r_t = 4.23$. 1H NMR (300 MHz, $CDCl_3$) δ_H 8.78 (m, 2H), 8.50 (m, 1H), 8.22 (s, 1H), 7.52 (m, 2H), 6.96 (s, 1H), 3.09 (s, 3H). HRMS (ESI) for $C_{11}H_{11}ClN_3O_2S$ $[M+H]^+$ calcd.: 284.0261, found: 284.0264.

4-(Pyridin-4-yl)-1H-indole, 8. A mixture of 4-bromo-1H-indole (70 mg, 0.36 mmol), 4-(4,4,5,5-tetramethyl-1,3,2-dioxaborolan-2-yl)pyridine (109 mg, 0.56 mmol), catalytic tetrakis(triphenylphosphine) palladium (0), sat. sodium bicarbonate (aq.) (1 mL) and DMF (2 mL) were combined in a microwave vial and heated at 160 °C for 30 min. The reaction was concentrated and separated between DCM and sat. sodium bicarbonate (aq.). The material was purified by MDAP (method B), then freeze-dried from 1,4-dioxane and water to give the title compound. LCMS (method B): 100%, $r_t = 2.08$, $[M+H]^+ = 195$. 1H NMR (600 MHz, DMSO- d_6) δ_H 11.64 (br. s., 1H), 8.87 (d, $J=4.9$ Hz, 2H), 8.16 (d, $J=6.0$ Hz, 2H), 7.64 (d, $J=7.9$ Hz, 1H), 7.59 (t, $J=2.6$ Hz, 1H), 7.40 (d, $J=7.2$ Hz, 1H), 7.25-7.33 (t, $J=7.7$ Hz, 1H), 6.73 (br. s., 1H). HRMS (ESI) for $C_{13}H_{11}N_2$ $[M+H]^+$ calcd.: 195.0923, found: 195.0930.

***N*-[2-Chloro-5-(7-isoquinolinyl)-3-pyridinyl]methanesulfonamide, 9.** 7-Isoquinolinylboronic acid (100 mg, 0.578 mmol), *N*-(5-bromo-2-chloropyridin-3-yl)methanesulfonamide (165 mg, 0.578 mmol), Tripotassium phosphate (368 mg, 1.734 mmol) and $PdCl_2dppf$ (32.4 mg, 0.058 mmol) were weighed to a microwave vial. The vial was sealed and 1,4-dioxane (4 mL) and water (1 mL) were added. The vial was then flushed with nitrogen and heated at 80 °C for 3 h. The residue was diluted with DCM (30 mL) and washed with brine (30 mL), then water (2 x 30 mL). The organic layer was then passed through a hydrophobic frit and evaporated to dryness. The residue was purified by MDAP (method A). Pure fractions were evaporated and combined to give the title

compound 35.9 mg (19% yield). LCMS (method A): 100%, $r_t = 0.52$, $[M+H]^+ = 334/336$. 1H NMR (400 MHz, DMSO- d_6) δ_H 9.42 (s, 1H), 8.73 (d, $J=2.5$ Hz, 1H), 8.51-8.59 (m, 2H), 8.25 (d, $J=2.3$ Hz, 1H), 8.09-8.19 (m, 3H), 7.89 (d, $J=5.8$ Hz, 1H), 3.17 (s, 3H). HRMS (ESI) for $C_{15}H_{13}ClN_3O_2S$ $[M+H]^+$ calcd.: 334.0418, found: 334.0418.

7-(1*H*-Indol-4-yl)isoquinoline, 10. In a microwave vial, 7-bromoisoquinoline (95 mg, 0.46 mmol), tripotassium phosphate (242 mg, 1.14 mmol) and indole-4-boronic acid (74 mg, 0.46 mmol) were partially dissolved into a two-phase mixture of CPME (8 mL) and water (2 mL). This was purged by bubbling a stream of nitrogen through it for 5 min. $PdCl_2(dppf)$ (34 mg, 0.046 mmol) was added and the reaction was heated at 140 °C for 30 min in a microwave. The reaction was diluted with DCM (60 mL) and water (20 mL) then the phases separated using a hydrophobic frit. The aqueous phase was extracted with further DCM (20 mL) then the combined organic phases were concentrated *in vacuo*. The residue was purified by MDAP (method C). Product fractions were combined and concentrated *in vacuo* to give the title compound, 56.6 mg (51% yield). LCMS (method C): 100%, $r_t = 1.04$, $[M+H]^+ = 245$. 1H NMR (400 MHz, DMSO- d_6) δ_H 11.37 (br. s., 1H), 9.42 (s, 1H), 8.53 (d, $J=5.8$ Hz, 1H), 8.40 (s, 1H), 8.07-8.16 (m, 2H), 7.89 (d, $J=5.8$ Hz, 1H), 7.46-7.52 (m, 2H), 7.22-7.29 (m, 2H), 6.68 (br. s., 1H). HRMS (ESI) for $C_{17}H_{13}N_2$ $[M+H]^+$ calcd.: 245.1080, found: 245.1083.

***N*-(2-Chloro-5-(3,6-dihydro-2*H*-pyran-4-yl)pyridin-3-yl)methanesulfonamide, 11.** A mixture of *N*-(2-chloro-5-(4,4,5,5-tetramethyl-1,3,2-dioxaborolan-2-yl)pyridin-3-yl)methanesulfonamide (797 mg, 2.4 mmol), 3,6-dihydro-2*H*-pyran-4-yl trifluoromethanesulfonate (464 mg, 2 mmol), $PdCl_2dppf$.DCM (163 mg, 0.2 mmol), sodium carbonate (530 mg, 5 mmol) in 1,4-dioxane (16 mL) and water (4 mL) was heated at 80 °C for 2 h. The mixture was filtered and the filtrate was concentrated. The residue was purified by silica chromatography, eluting with ethyl acetate: petroleum ether (1:5, v/v). The material was washed with ethyl acetate (5 mL), filtered, washed with further ethyl acetate, then dried *in vacuo* to give the title compound 245 mg (45% yield). HPLC (method B): 99.6%, $r_t = 6.25$. 1H NMR (300 MHz, $CDCl_3$) δ_H 8.26 (d, $J=2.4$ Hz, 1H), 7.98 (d, $J=2.4$ Hz, 1H), 6.78 (s, 1H), 6.28 (s, 1H), 4.33-4.36 (m, 2H), 3.95 (t, $J=5.4$ Hz, 2H), 3.07 (s, 3H), 2.50-2.53 (m, 2H). HRMS (ESI) for $C_{11}H_{14}ClN_2O_3S$ $[M+H]^+$ calcd.: 289.0414, found: 289.0418.

***N*-(5-(2-Aminopyrimidin-5-yl)-2-chloropyridin-3-yl)methanesulfonamide, 12.** A mixture of *N*-(2-chloro-5-(4,4,5,5-tetramethyl-1,3,2-dioxaborolan-2-yl)pyridin-3-yl)methanesulfonamide (40 mg, 0.12 mmol), 5-bromopyrimidin-2-amine (21 mg, 0.12 mmol), tripotassium phosphate (76 mg, 0.36 mmol), chloro(di-2-norbornylphosphino)(2'-dimethylamino-1,1'-biphenyl-2-yl)palladium(II) (7 mg, 0.012 mmol) in 1,4-dioxane (0.8 mL) and water (0.2 mL) were heated in a sealed tube in a microwave at 120 °C for 20 min. The mixture was

loaded onto a C₁₈ SPE cartridge (pre-conditioned with acetonitrile containing 0.1% TFA), and washed through with acetonitrile containing 0.1% TFA (3 mL). The solvent was removed under a flow of nitrogen. The residue was purified by MDAP (method D). The solvent was dried under a stream of nitrogen to give the title compound 4.2 mg (9% yield). LCMS (method C): 100%, rt = 0.51, [M+H]⁺ = 300/302. ¹H NMR (600 MHz, DMSO-d₆) δ_H 8.62 (s, 2H), 8.45 (d, J=2.3 Hz, 1H), 7.99 (d, J=2.3 Hz, 1H), 6.98 (s, 2H), 3.12 (s, 3H). HRMS (ESI) for C₁₀H₁₁ClN₅O₂S [M+H]⁺ calcd.: 300.0323, found: 300.0328.

***N*-(2-Chloro-5-(3,6-dihydro-2H-pyran-4-yl)pyridin-3-yl)benzenesulfonamide, 13.** A mixture of *N*-(2-chloro-5-(4,4,5,5-tetramethyl-1,3,2-dioxaborolan-2-yl)pyridin-3-yl)benzenesulfonamide (946 mg, 2.4 mmol), 3,6-dihydro-2H-pyran-4-yl trifluoromethanesulfonate (464 mg, 2 mmol), PdCl₂dppf.DCM (163 mg, 0.2 mmol), sodium carbonate (530 mg, 5 mmol) in 1,4-dioxane (16 mL) and water (4 mL) was heated at 80 °C for 2 h under nitrogen. The mixture was filtered and the filtrate was concentrated. The residue was purified by silica chromatography, eluting with ethyl acetate: petroleum ether (1:5, v/v). The material was washed with ethyl acetate (5 mL), filtered, washed with further ethyl acetate, then dried *in vacuo*. The residue was further purified by preparative-HPLC to give the title compound 287 mg (41% yield). HPLC (method C): 98.9%, rt = 5.97. ¹H NMR (300 MHz, DMSO-d₆) δ_H 10.33 (s, 1H), 8.34 (d, J=2.4 Hz, 1H), 7.56-7.74 (m, 6H), 6.37 (s, 1H), 4.22 (m, 2H), 3.81 (t, J=5.4 Hz, 2H), 2.36-2.51 (m, 2H). HRMS (ESI) for C₁₆H₁₆ClN₂O₃S [M+H]⁺ calcd.: 351.0571, found: 351.0576.

***N*-(2-Chloro-5-phenylpyridin-3-yl)benzenesulfonamide, 14.** To a solution of *N*-(5-bromo-2-chloropyridin-3-yl)benzenesulfonamide (200 mg, 0.57 mmol) and phenylboronic acid (63 mg, 0.52 mmol) in 1,4-dioxane (10 mL) and water (5 mL) was added potassium carbonate (216 mg, 1.56 mmol) and the mixture was degassed. Tetrakis(triphenylphosphine) palladium (0) was added and the reaction was refluxed for 13 hours. The reaction was extracted with ethyl acetate, the organic layer was washed with brine, dried over magnesium sulfate, filtered and evaporated. The residue was purified by silica chromatography using 10% ethyl acetate in DCM, followed by reverse-phase purification using acetonitrile: water (1:1, v/v) to give the title compound, 50 mg (28% yield). LCMS (method B): 100%, rt = 1.15, [M+H]⁺ = 345/347. ¹H NMR (400 MHz, Methanol-d₄) δ_H 8.43 (d, J=2.3 Hz, 1H), 8.16 (d, J=2.3 Hz, 1H), 7.80-7.84 (m, 2H), 7.61-7.68 (m, 3H), 7.50-7.57 (m, 4H), 7.44-7.50 (m, 1H). HRMS (ESI) for C₁₇H₁₄ClN₂O₂S [M+H]⁺ calcd.: 345.0465, found: 345.0467.

***N*-(5-(3,6-Dihydro-2H-pyran-4-yl)-2-methoxypyridin-3-yl)benzenesulfonamide, 15.** 5-(3,6-Dihydro-2H-pyran-4-yl)-2-methoxypyridin-3-amine (compound S7, 105 mg, 0.509 mmol) was dissolved in pyridine (2 mL)

and benzenesulfonyl chloride (0.066 mL, 0.509 mmol) was added. The reaction was stirred at room temperature overnight. The reaction was evaporated to dryness. Half the material was dissolved in DMSO: methanol (1 mL, 1:1, v/v) and purified by MDAP (method A). Product containing fraction was evaporated to dryness to give title compound 61 mg (35% yield). LCMS (method A): 100%, $r_t = 0.94$, $[M+H]^+ = 347$. 1H NMR (400 MHz, DMSO- d_6) δ_H 9.85 (s, 1H), 8.00 (d, $J=2.3$ Hz, 1H), 7.71-7.76 (m, 2H), 7.60-7.66 (m, 2H), 7.53-7.59 (m, 2H), 6.14 (tt, $J=1.6, 3.1$ Hz, 1H), 4.21 (q, $J=2.8$ Hz, 2H), 3.81 (t, $J=5.4$ Hz, 2H), 3.61 (s, 3H), 2.37 (dt, $J=2.8, 5.0$ Hz, 2H). HRMS (ESI) for $C_{17}H_{19}N_2O_4S$ $[M+H]^+$ calcd.: 347.1066, found: 347.1068.

1-Benzyl-*N*-(5-(3,6-dihydro-2*H*-pyran-4-yl)-2-methoxypyridin-3-yl)-2-methyl-1*H*-imidazole-4-

sulfonamide, 16. (Bromomethyl)benzene (0.05 mL, 0.414 mmol) was added to *N*-(5-(3,6-dihydro-2*H*-pyran-4-yl)-2-methoxypyridin-3-yl)-*N*-(4-methoxybenzyl)-2-methyl-1*H*-imidazole-5-sulfonamide (compound **S9**, 130 mg, 0.276 mmol) and potassium carbonate (57.3 mg, 0.414 mmol) in DMF (1 mL) and stirred at room temperature over the weekend. The reaction was quenched with water (3 mL). Ethyl acetate (5 mL) was added and the aqueous was separated and washed with ethyl acetate (3 mL). The combined organics were washed with 7.5% LiCl (aq.) (3 mL x 2), water (3 mL), brine (3mL), then separated, passed through a hydrophobic frit and dried under a stream of nitrogen. DCM (1 mL) and TFA (0.5 mL) were added to the residue and the reaction was stirred overnight at room temperature, then transferred to a microwave vial and heated in the microwave at 80 °C for a total of 30 min. The reaction was added cautiously to sat. sodium bicarbonate (aq.) (4 mL) and diluted with DCM. The DCM was passed through a hydrophobic frit then evaporated to dryness. The residue was dissolved in DMSO: methanol (1 mL, 1:1, v/v), filtered and purified by MDAP (method A). Product containing fraction was evaporated under a stream of nitrogen to give the title compound, 18 mg, (15% yield). LCMS (method A): 100%, $r_t = 0.91$, $[M+H]^+ = 441$. 1H NMR (600 MHz, DMSO- d_6) δ_H ppm 9.46 (br. s, 1H), 7.96 (d, $J=1.5$ Hz, 1H), 7.80 (s, 1H), 7.76 (d, $J=2.2$ Hz, 1H), 7.28 - 7.37 (m, 3H), 7.09 (d, $J=7.3$ Hz, 2H), 6.12 (br. s, 1H), 5.18 (s, 2H), 4.19 (q, $J=2.8$ Hz, 2H), 3.79 (t, $J=5.5$ Hz, 2H), 3.74 (s, 3H), 2.36 (td, $J=5.2, 2.8$ Hz, 2H), 2.23 (s, 3 H). ^{13}C (151 MHz, DMSO- d_6) δ_C ppm 155.8, 146.8, 136.7, 130.6, 129.32, 129.30, 129.28, 129.2, 128.4, 127.6, 125.6, 122.8, 114.6, 65.5, 64.0, 55.6, 53.8, 49.6, 26.7, 13.3. HRMS (ESI) for $C_{22}H_{25}N_4O_4S$ $[M+H]^+$ calcd.: 441.1597, found: 441.1596.

Biology. PI3K α , - β , - γ , and - δ HTRF Assays. Inhibition of PI3Kinase enzymatic activity was determined using a homogeneous time-resolved fluorescence (HTRF) kit assay format provided by Millipore. Reactions were performed in assay buffer containing 50 mM HEPES, pH 7.0, 150 mM NaCl, 10 mM MgCl₂, <1% cholate (w/v), <1% CHAPS (w/v), 0.05% sodium azide (w/v), and 1 mM DTT. Enzymes were preincubated with compound,

serially diluted 4-fold in 100% DMSO, for 15 min prior to reaction initiation upon addition of substrate solution containing ATP at K_m for the specific isoform tested (α at 250 μ M, β at 400 μ M, δ at 80 μ M, and γ at 15 μ M), PIP2 at either 5 μ M (PI3K δ) or 8 μ M (PI3K α , - β , and - γ) and 10 nM biotin-PIP3. Assays were quenched after 60 min by addition of a quench/detection solution prepared in 50 mM HEPES, pH 7.0, 150 mM NaCl, <1% cholate, <1% Tween 20, 30 mM EDTA, 40 mM potassium fluoride, and 1 mM DTT containing 16.5 nM GRP-1 PH domain, 8.3 nM streptavidin-APC, and 2 nM europium-anti-GST and were left for a further 60 min in the dark to equilibrate prior to reading using a BMG RubyStar plate reader. Ratio data were normalized to high (no compound) and low (no enzyme) controls prior to fitting using a logistical four-parameter equation to determine IC_{50} . Ligand efficiency was calculated according to³⁰.

Ancillary Information

Supporting Information Availability

The Supporting Information is available free of charge on the ACS Publications website.

Molecular formula strings

Crystallography methods

Chemistry methods

Assay methods for data on compound 16

Kinase screening data for compounds 7 and 16

Free-Wilson analysis, coverage and correlation plots

Abbreviations

CLND, chemiluminescent nitrogen detection; CPME, cyclopentyl methyl ether; HTRF, homogeneous time resolved fluorescence; MDAP, mass directed automated preparative HPLC; MDCK, Madin-Darby canine kidney; MIP, molecular interaction potential.

Author Information

Corresponding Author

*E-mail: Kenneth.d.down@gsk.com. Telephone: 00441438762042.

§Present address: Charles River, Chesterford Research Park, Saffron Walden, Essex, CB10 1XL, UK.

Notes

The authors declare the following competing financial interest(s): All authors were employees of GlaxoSmithKline at the time the work was carried out.

Acknowledgements

The authors thank members of Protein & Cellular Sciences, PTS, GSK, for protein production; Damien Bonvalot, Aurelie Champigny, Paul Cox, G. Huang, J. Kaspavec, X. Lui, Susan Macintyre, Elvis Maduli, David Perez, Andy Philp and Xiangsheng Li for their synthetic chemistry contributions; and Colin Edge and Zoë Henley for review of the manuscript.

Accession Codes

Coordinates have been deposited with the Protein Data Bank with accession codes XXX, XXX & XXX.

References

1. Cantley, L. C., The phosphoinositide 3-kinase pathway. *Science* **2002**, 296 (5573), 1655-1657.

2. Vanhaesebroeck, B.; Guillermet-Guibert, J.; Graupera, M.; Bilanges, B., The emerging mechanisms of isoform-specific PI3K signalling. *Nat Rev Mol Cell Biol* **2010**, *11* (5), 329-341.
3. Foster, J. G.; Blunt, M. D.; Carter, E.; Ward, S. G., Inhibition of PI3K signaling spurs new therapeutic opportunities in inflammatory/autoimmune diseases and hematological malignancies. *Pharmacol Rev* **2012**, *64* (4), 1027-1054.
4. Engelman, J. A.; Luo, J.; Cantley, L. C., The evolution of phosphatidylinositol 3-kinases as regulators of growth and metabolism. *Nat Rev Genet* **2006**, *7* (8), 606-619.
5. McNamara, C. R.; Degterev, A., Small-Molecule Inhibitors of the PI3K Signaling Network. In *Future Medicinal Chemistry*, Future Science: 2011; Vol. 3, pp 549-565.
6. Vanhaesebroeck, B.; Ali, K.; Bilancio, A.; Geering, B.; Foukas, L. C., Signalling by PI3K isoforms: insights from gene-targeted mice. *Trends Biochem Sci* **2005**, *30* (4), 194-204.
7. Rowan, W. C.; Smith, J. L.; Affleck, K.; Amour, A., Targeting phosphoinositide 3-kinase delta for allergic asthma. *Biochem Soc Trans* **2012**, *40* (1), 240-245.
8. Sriskantharajah, S.; Hamblin, N.; Worsley, S.; Calver, A. R.; Hessel, E. M.; Amour, A., Targeting phosphoinositide 3-kinase delta for the treatment of respiratory diseases. *Ann N Y Acad Sci* **2013**, *1280*, 35-39.
9. Norman, P., Selective PI3K δ inhibitors, a review of the patent literature. *Expert Opinion on Therapeutic Patents* **2011**, *21* (11), 1773-1790.
10. A. Sabbah, D.; Hu, J.; A. Zhong, H., Advances in the development of class I phosphoinositide 3-kinase (PI3K) inhibitors. *Current Topics in Medicinal Chemistry* **2016**, *16* (13), 1413-1426.
11. Dienstmann, R.; Rodon, J.; Serra, V.; Tabernero, J., Picking the point of inhibition: a comparative review of PI3K/AKT/mTOR pathway inhibitors. *Mol Cancer Ther* **2014**, *13* (5), 1021-1031.
12. Shin, Y.; Suchomel, J.; Cardozo, M.; Duquette, J.; He, X.; Henne, K.; Hu, Y. L.; Kelly, R. C.; McCarter, J.; McGee, L. R.; Medina, J. C.; Metz, D.; San Miguel, T.; Mohn, D.; Tran, T.; Vissinga, C.; Wong, S.; Wannberg, S.; Whittington, D. A.; Whoriskey, J.; Yu, G.; Zalameda, L.; Zhang, X.; Cushing, T. D., Discovery, optimization, and in vivo evaluation of benzimidazole derivatives AM-8508 and AM-9635 as potent and selective PI3K δ inhibitors. *J Med Chem* **2016**, *59* (1), 431-447.
13. Hoegenauer, K.; Soldermann, N.; Zecri, F.; Strang, R. S.; Graveleau, N.; Wolf, R. M.; Cooke, N. G.; Smith, A. B.; Hollingworth, G. J.; Blanz, J.; Gutmann, S.; Rummel, G.; Littlewood-Evans, A.; Burkhart, C., Discovery of CDZ173 (leniolisib), representing a structurally novel class of PI3K delta-selective inhibitors. *ACS Med Chem Lett* **2017**, *8* (9), 975-980.

14. Allen, R. A.; Brookings, D. C.; Powell, M. J.; Delgado, J.; Shuttleworth, L. K.; Merriman, M.; Fahy, I. J.; Tewari, R.; Silva, J. P.; Healy, L. J.; Davies, G. C. G.; Twomey, B.; Cutler, R. M.; Kotian, A.; Crosby, A.; McCluskey, G.; Watt, G. F.; Payne, A., Seletalisib: Characterization of a novel, potent, and selective inhibitor of PI3Kdelta. *J Pharmacol Exp Ther* **2017**, *361* (3), 429-440.
15. Down, K.; Amour, A.; Baldwin, I. R.; Cooper, A. W.; Deakin, A. M.; Felton, L. M.; Guntrip, S. B.; Hardy, C.; Harrison, Z. A.; Jones, K. L.; Jones, P.; Keeling, S. E.; Le, J.; Livia, S.; Lucas, F.; Lunniss, C. J.; Parr, N. J.; Robinson, E.; Rowland, P.; Smith, S.; Thomas, D. A.; Vitulli, G.; Washio, Y.; Hamblin, J. N., Optimization of novel indazoles as highly potent and selective inhibitors of phosphoinositide 3-kinase delta for the treatment of respiratory disease. *J Med Chem* **2015**, *58* (18), 7381-7399.
16. Cahn, A.; Hamblin, J. N.; Begg, M.; Wilson, R.; Dunsire, L.; Sriskantharajah, S.; Montembault, M.; Leemereise, C. N.; Galinanes-Garcia, L.; Watz, H.; Kirsten, A. M.; Fuhr, R.; Hessel, E. M., Safety, pharmacokinetics and dose-response characteristics of GSK2269557, an inhaled PI3Kdelta inhibitor under development for the treatment of COPD. *Pulm Pharmacol Ther* **2017**, *46*, 69-77.
17. <https://clinicaltrials.gov/ct2/show/NCT02294734> (accessed July 25, 2018).
18. <https://clinicaltrials.gov/ct2/show/NCT03345407> (accessed July 25, 2018).
19. <https://clinicaltrials.gov/ct2/show/NCT03045887> (accessed July 25, 2018).
20. Amour, A.; Barton, N.; Cooper, A. W.; Inglis, G.; Jamieson, C.; Luscombe, C. N.; Morrell, J.; Peace, S.; Perez, D.; Rowland, P.; Tame, C.; Uddin, S.; Vitulli, G.; Wellaway, N., Evolution of a novel, orally bioavailable series of PI3Kdelta inhibitors from an inhaled lead for the treatment of respiratory disease. *J Med Chem* **2016**, *59* (15), 7239-7251.
21. Sutherlin, D. P.; Baker, S.; Bisconte, A.; Blaney, P. M.; Brown, A.; Chan, B. K.; Chantry, D.; Castanedo, G.; DePledge, P.; Goldsmith, P.; Goldstein, D. M.; Hancox, T.; Kaur, J.; Knowles, D.; Kondru, R.; Lesnick, J.; Lucas, M. C.; Lewis, C.; Murray, J.; Nadin, A. J.; Nonomiya, J.; Pang, J.; Pegg, N.; Price, S.; Reif, K.; Safina, B. S.; Salphati, L.; Staben, S.; Seward, E. M.; Shuttleworth, S.; Sohal, S.; Sweeney, Z. K.; Ultsch, M.; Waszkowycz, B.; Wei, B., Potent and selective inhibitors of PI3Kδ: Obtaining isoform selectivity from the affinity pocket and tryptophan shelf. *Bioorganic & Medicinal Chemistry Letters* **2012**, *22* (13), 4296-4302.
22. Andrs, M.; Korabecny, J.; Jun, D.; Hodny, Z.; Bartek, J.; Kuca, K., Phosphatidylinositol 3-Kinase (PI3K) and phosphatidylinositol 3-kinase-related kinase (PIKK) inhibitors: importance of the morpholine ring. *J Med Chem* **2015**, *58* (1), 41-71.

23. Cheeseright, T. J.; Mackey, M. D.; Melville, J. L.; Vinter, J. G., FieldScreen: virtual screening using molecular fields. Application to the DUD data set. *J Chem Inf Model* **2008**, *48* (11), 2108-2117.
24. Free, S. M.; Wilson, J. W., A mathematical contribution to structure-activity studies. *Journal of Medicinal Chemistry* **1964**, *7* (4), 395-399.
25. Yang, H. W.; Craven, B. M., Charge density study of 2-pyridone. *Acta Crystallographica Section B Structural Science* **1998**, *54* (6), 912-920.
26. Berndt, A.; Miller, S.; Williams, O.; Le, D. D.; Houseman, B. T.; Pacold, J. I.; Gorrec, F.; Hon, W.-C.; Ren, P.; Liu, Y.; Rommel, C.; Gaillard, P.; Ruckle, T.; Schwarz, M. K.; Shokat, K. M.; Shaw, J. P.; Williams, R. L., The p110[delta] structure: mechanisms for selectivity and potency of new PI(3)K inhibitors. *Nat Chem Biol* **2010**, *6* (2), 117-124.
27. D'Angelo, N. D.; Kim, T. S.; Andrews, K.; Booker, S. K.; Caenepeel, S.; Chen, K.; D'Amico, D.; Freeman, D.; Jiang, J.; Liu, L.; McCarter, J. D.; San Miguel, T.; Mullady, E. L.; Schrag, M.; Subramanian, R.; Tang, J.; Wahl, R. C.; Wang, L.; Whittington, D. A.; Wu, T.; Xi, N.; Xu, Y.; Yakowec, P.; Yang, K.; Zalameda, L. P.; Zhang, N.; Hughes, P.; Norman, M. H., Discovery and optimization of a series of benzothiazole phosphoinositide 3-kinase (PI3K)/mammalian target of rapamycin (mTOR) dual inhibitors. *J Med Chem* **2011**, *54* (6), 1789-1811.
28. Nishimura, N.; Siegmund, A.; Liu, L.; Yang, K.; Bryan, M. C.; Andrews, K. L.; Bo, Y.; Booker, S. K.; Caenepeel, S.; Freeman, D.; Liao, H.; McCarter, J.; Mullady, E. L.; San Miguel, T.; Subramanian, R.; Tamayo, N.; Wang, L.; Whittington, D. A.; Zalameda, L.; Zhang, N.; Hughes, P. E.; Norman, M. H., Phosphoinositide 3-kinase (PI3K)/mammalian target of rapamycin (mTOR) dual inhibitors: discovery and structure-activity relationships of a series of quinoline and quinoxaline derivatives. *J Med Chem* **2011**, *54* (13), 4735-4751.
29. Knight, S. D.; Adams, N. D.; Burgess, J. L.; Chaudhari, A. M.; Darcy, M. G.; Donatelli, C. A.; Luengo, J. I.; Newlander, K. A.; Parrish, C. A.; Ridgers, L. H.; Sarpong, M. A.; Schmidt, S. J.; Van Aller, G. S.; Carson, J. D.; Diamond, M. A.; Elkins, P. A.; Gardiner, C. M.; Garver, E.; Gilbert, S. A.; Gontarek, R. R.; Jackson, J. R.; Kershner, K. L.; Luo, L.; Raha, K.; Sherk, C. S.; Sung, C.-M.; Sutton, D.; Tummino, P. J.; Wegrzyn, R. J.; Auger, K. R.; Dhanak, D., Discovery of GSK2126458, a highly potent inhibitor of PI3K and the mammalian target of rapamycin. *ACS Medicinal Chemistry Letters* **2010**, *1* (1), 39-43.
30. Hopkins, A. L.; Groom, C. R.; Alex, A. Ligand efficiency: a useful metric for lead selection. *Drug Discovery Today* **2004**, *9*, 430-431.

Table of Contents graphic

